

Active Disturbance Rejection Control Design for Trajectory Tracking of Parafoil and Payload System

Pan-long Tan¹ Qing-lin Sun¹ Er-lin Zhu¹ Zeng-qiang Chen¹

¹ Intelligent Robots Key Lab of Tianjin, College of Computer and Control Engineering,
Nankai University
Tianjin 300071, China
sunql@nankai.edu.cn

Received 30 September 2008; Revised 26 November 2015; Accepted 8 January 2016

Abstract. This paper presents the design and implementation of the trajectory tracking controller for the parafoil and payload system. The controller is developed based on the active disturbance rejection control (ADRC) algorithm and is adequate to cope with the nonlinear dynamics of the parafoil and payload system and the disturbances. Horizontal and vertical control channels are design for the parafoil and payload system to track the desired trajectory. Simulations and comparisons are utilized to illustrate the effectiveness and advantage of ADRC. Wind disturbances of both stable and NASA wind gust model are added to the simulations as external disturbances. A tuning method for discrete ADRC controller to adapt different sampling rate is proposed, which simplifies the tuning procedure of the control system with adjustable sampling rate.

Keywords: ADRC, Parafoil and payload system, Trajectory tracking

1 Introduction

In general, the parachute systems, round parachutes and parafoil systems, are often used in high atmosphere recovery missions. The parafoil system is developed from traditional round parachute. The main difference between the two types of parachutes is that the round parachute is body falling under gravity forces and air friction while parafoil system is a kind of gliding aircraft, since it has the capability of lift force generation [1]. The parafoil system is steerable and is given a guidance capability for recovery purposes. The steerability enables parafoil system to achieve precise landing and avoid turbulence zones and dangerous landing area during the descent [2].

The parafoil and payload system consists of a parafoil and a suspended payload body equipped with an engine and a propeller [3]. Controllable parafoil and payload system is controlled with downward deflection of left and right parafoil breaks as well as thrust of the propeller. The fly direction and horizontal plane position of parafoil and payload system is determined by left and right deflection while the vertical velocity is determined by thrust. Several autonomous parafoil and payload system have been studied and developed for various purposes such as land observation, surveillance, and reconnaissance of the ground circumstances.

The trajectory tracking problem of aircraft is now still a challenging one because of the nonlinear dynamics of aircraft and external disturbances, especially for the parafoil and payload system [4]. Since the parafoil is made of fabric and is easily influenced by air flow. For many years, unpowered parafoil systems are controlled by conventional control method, but the control of powered parafoil system is seldom introduced. LIU proposed a hybrid algorithm of fuzzy control and predictive control method in his paper in flight path tracking of parafoil gliding system [5]. It is very complicated to tune system parameters of the hybrid algorithm, and the controller is relatively time-consuming. Slegers and Costello applied the Model Predictive Control (MPC) method in the horizontal path tracking based on an invariant reduced order model of parafoil and payload system [6]. Altitude control is not introduced in the paper. And the invariant reduced order model based MPC is inadequate to adapt to changeable wind disturbance.

The work reported here applied active disturbance rejection control (ADRC) to the parafoil and payload system to control horizontal trajectory and vertical altitude. The ADRC is proposed by Han based on feedback linearization approach [7]. The basic idea of ADRC is to use an extended state observer (ESO) to track system dynamics and the total disturbance in real time and dynamically compensate for it.

To get precise position information in real time, the global positioning system (GPS) module is equipped to the parafoil and payload system. The sampling rate of GPS directly affect the performance of trajectory tracking controller. Although higher sampling rate brings better tracking and response performance, the system becomes energy consuming because of the frequent operation of motors. Therefore, tuning ADRC parameters to adapt

different GPS sampling rate for a parafoil and payload system to achieve diverse tasks become a problem to be solved. A tuning method for ADRC parameters to adapt different sampling rate is presented in this paper.

2 Active Disturbance Rejection Control

To overcome the limitations of PID and the model-based intelligent control algorithm, Han proposed the concept and method of ADRC based on feedback linearization approach [8]. It is well known that feedback control is to deal with the variations and uncertainties of the system dynamics and unknown disturbance.

As the aim of this paper is to control the horizontal and vertical position of the parafoil and payload system, following the desired path, thus the dynamic model of the parafoil and payload system is considered as a second order nonlinear system in ADRC analysis. The detailed modeling procedure is shown in [9], in which we focused on the modeling problem of parafoil and payload system. The second order system is described as

$$\ddot{y} = -a_1\dot{y} - a_2y + \omega + bu \quad (1)$$

Where y is the output, u is the input and ω is the external disturbance. a_1 , a_2 and b denote system parameters.

Then rewrite the system function as

$$\ddot{y} = -a_1\dot{y} - a_2y + \omega + (b - b_0)u + b_0u = f(t, y, \dot{y}, \omega) + b_0u \quad (2)$$

$$f(t, y, \dot{y}, \omega) = -a_1\dot{y} - a_2y + \omega + (b - b_0)u \quad (3)$$

Where $f(t, y, \dot{y}, \omega)$ represents internal dynamics $-a_1\dot{y} - a_2y + (b - b_0)u$ and the external disturbance ω .

The basic idea of ADRC is to obtain \hat{f} , the estimation of f , and use it in the control law. Let $u = (-\hat{f} + u_0)/b_0$ and the system is reduced to a unit gain double integrator control system, $\ddot{y} = (f - \hat{f}) + u_0$.

Let $h = \dot{f}(t, y, \dot{y}, \omega)$ and system (1) is rewritten in the state equation form

$$\begin{cases} \dot{x}_1 = x_2 \\ \dot{x}_2 = x_3 + b_0u \\ \dot{x}_3 = h \\ y = x_1 \end{cases} \quad (4)$$

Where $x_3 = f$ is added as an augmented state. Then f can be estimated by using the state observer based on state space model

$$\begin{cases} \dot{x} = Ax + Bu + Eh \\ y = Cx \end{cases} \quad (5)$$

Where

$$A = \begin{bmatrix} 0 & 1 & 0 \\ 0 & 0 & 1 \\ 0 & 0 & 0 \end{bmatrix}, B = \begin{bmatrix} 0 \\ b \\ 0 \end{bmatrix}, C = [1 \ 0 \ 0], E = \begin{bmatrix} 0 \\ 0 \\ 1 \end{bmatrix} \quad (6)$$

Then the extended state observer (ESO) of the second order system is constructed as

$$\begin{cases} \dot{z} = Az + Bu + L(y - \hat{y}) \\ \hat{y} = Cz \end{cases} \quad (7)$$

And L is the observer gain vector

$$L = [\beta_1 \ \beta_2 \ \beta_3]^T \quad (8)$$

Where the superscript T denotes transpose. As shown in [10], the selection of the observer gain is formulated as

$$\beta_1 = 3\omega_o, \beta_2 = 3\omega_o^2, \beta_3 = \omega_o^3 \quad (9)$$

It results in characteristic polynomial of ESO to be

$$\lambda(s) = s^3 + 3s^2\omega_o + 3s\omega_o^2 + \omega_o^3 = (s + \omega_o)^3 \quad (10)$$

The ω_o denotes the parameter to be tuned which indicates the bandwidth of ESO [10]. The bandwidth parameterization greatly simplifies the observer designing and tuning by making all observer gains a function of the observer gain ω_o .

With the ESO properly designed, z_3 precisely estimates f and the controller output is given as

$$u = \frac{-z_3 + u_0}{b_0} \quad (11)$$

Ignoring the estimation error of z_3 , the system model is reduced to unit-gain double integrator control system

$$\ddot{y} = (f - z_3) + u_0 \approx u_0 \quad (12)$$

As a result, the system becomes a much easier control problem that is easy to deal with. A simple PD controller is usually sufficient for the system. The PD controller is designed in the form of

$$u_0 = k_p(r - z_1) - k_d z_2 \quad (13)$$

Where k_p and k_d denote parameters of the PD controller that can be set as

$$k_p = \omega_c^2 \quad k_d = 2\xi\omega_c \quad (14)$$

Which yields an approximate closed-loop transfer function

$$G = \frac{\omega_c^2}{s^2 + 2\xi\omega_c s + \omega_c^2} \quad (15)$$

Where ω_c and ξ are the desired closed-loop natural frequency and damping ratio, respectively. And ξ is selected to avoid output oscillations.

The block diagram of the ADRC method is organized as follows in Fig. 1.

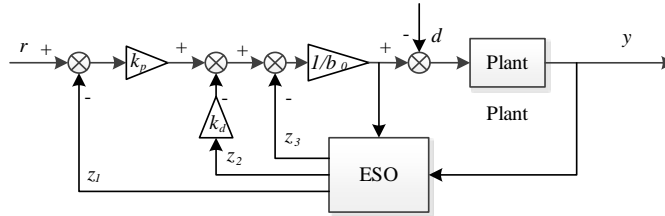


Fig. 1. ADRC block diagram

3 Designing of ADRC controllers

The position of parafoil and payload system consist of longitude, latitude, and altitude. As introduced in former sections, deflection and thrust are two input signals of the parafoil and payload system [9]. Thus, according to the engineering practice, two control channels are designed to control vertical and horizontal position of parafoil and payload system. The deflection is used to control fly direction and thrust is applied to vertical speed and altitude. The system diagram is shown in Fig. 2.

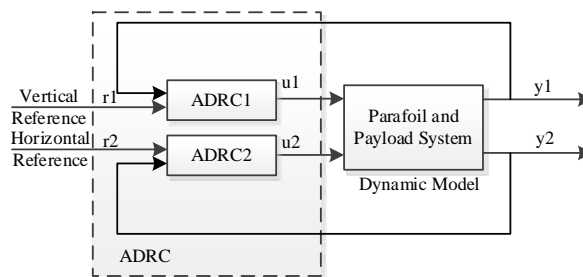


Fig. 2. Control block diagram of parafoil and payload system

In the figure, r_1 and r_2 are vertical altitude reference and horizontal reference of the desired path, respectively. u_1 denotes thrust signal and y_1 denotes the altitude of the parafoil and payload system. u_2 is the deflection of parafoil and y_2 is the fly direction of the parafoil and payload system.

3.1 Vertical altitude controller

The output of vertical ADRC altitude controller is the thrust control signal. The control signal is applied to drive the engine installed on the payload. The thrust acted on payload accelerate the parafoil and payload system and increase attack angle of the parafoil. If the thrust is increased over a critical value, the parafoil and payload system stops gliding downward and starts climbing.

The reference value of the vertical control is the altitude of the desired path. The difference between desired altitude and real system position is computed as the vertical error.

3.2 Horizontal trajectory tracking controller

The deflection control signal is the output of horizontal ADRC trajectory tracking controller and it is used to control the fly direction of the parafoil. The deflection is acted on the trailing edge of parafoil. When deflection is performed on the left trailing edge, the drag force on the left increased rapidly, and the parafoil turns left as a result and vice versa. The horizontal reference is horizontal trajectory, which is the projection of the desired path in the horizontal plane. The input of horizontal controller is the direction of horizontal trajectory. The difference between the fly direction of parafoil and payload system and the direction of the horizontal trajectory is used as the horizontal error. The horizontal distance between the parafoil system and the horizontal trajectory is treated as external disturbance which can be actively rejected by vertical ADRC controller.

4 Simulation results

To introduce ADRC application in trajectory tracking of the parafoil and payload system, simulation examples are presented in this paper. As parafoil is made of light fabric and is inflated by air, it is easily impacted by the wind. Wind disturbance affects the relative velocity between the parafoil and the air and finally affects parafoil dynamics by changing lift and drag force of it. Therefore, the wind disturbance is added to the parafoil and payload system in the simulation.

4.1 Tracking a circular trajectory with stable wind disturbance

The desired trajectory is a circle in the horizontal plane with a desired altitude. The desired altitude is set to be 1950 m and the start point of parafoil and payload system is set at (0, -300, 2000) m in the inertial coordinate system. The center of the circle is selected to be (0, 0, 2000) m in the horizontal plane and the radius of it is set to be 250 m. The sampling rate of GPS is 4 Hz. In addition, a comparison between ADRC and generalized predictive control (GPC) is presented in Fig. 3 and Fig. 5 to illustrate characteristics of ADRC.

A 3 m/s cross wind is added to the control system as external disturbance. The ADRC parameters for vertical altitude control channel 1 are tuned to be

$$\omega_{o1} = 3, \omega_{c1} = 0.2, b_{01} = 0.02 \quad (16)$$

The ADRC parameters for horizontal trajectory tracking control channel 2 are tuned to be

$$\omega_{o2} = 3, \omega_{c2} = 0.21, b_{02} = 0.05 \tag{17}$$

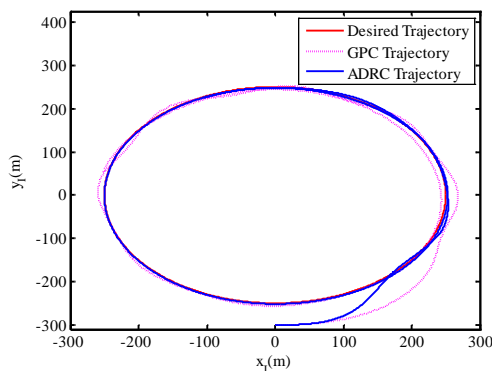


Fig. 3. Horizontal trajectory tracking

Fig. 3 shows the tracking performance of ADRC and GPC controllers in the horizontal plane. The performance of ADRC controller reveals more stable performance with a smooth trajectory and smaller tracking error. The settling time of ADRC controller is 68s and as a comparison, the settling time of GPC controller is 143s. The wind disturbance is apparently rejected by ADRC is a short time.

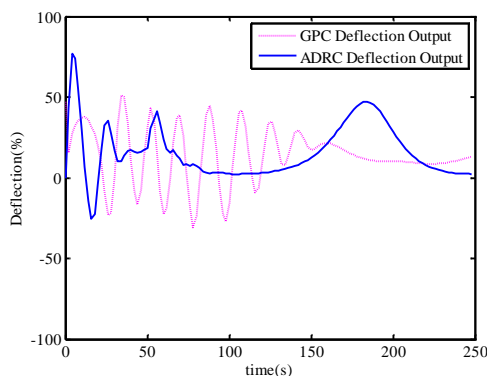


Fig. 4. Deflection output of controllers

Fig. 4 is a comparison of deflection between ADRC and GPC controllers and the figure confirms the performance comparison in Fig. 3. The deflection output of GPC controller vibrates in a large range at high frequency and slowly steady down to the smooth signal. The changing of deflection after 170s is caused by the stable cross wind disturbance. Compared to GPC controller, the ADRC controller is energy saving, and the deflection output of ADRC is comparatively smooth. The small vibration amplitude means less energy consumption.

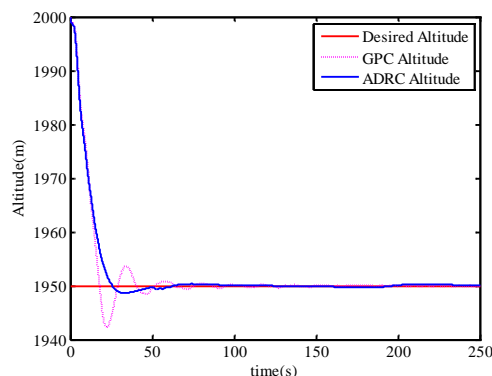


Fig. 5. Vertical altitude tracking

Fig. 5 denotes performance comparison between ADRC and GPC controllers in vertical altitude control. The overshoot of GPC controlled system is 7.8 m while that of ADRC controlled system is only 1.3 m. It also can be concluded from Fig. 5 that the settling time of GPC controller is 142s and is much longer than that of ADRC controller, 68s.

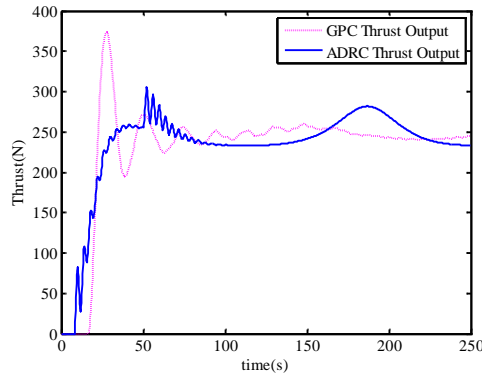


Fig. 6. Thrust output of controllers

Fig. 6 presents the thrust output of ADRC and GPC controllers.

As is shown in Fig. 3 and Fig. 5, the conclusion that ADRC is an effective way for trajectory tracking in both horizontal and vertical control channel can be obtained. It also can be concluded from the comparison that ADRC outperforms GPC.

4.2 Tracking a circle path with different sampling rate

In the discrete application, the value $\omega_o T$ determines the ESO performance [11]. T denotes system sampling rate. When an ADRC controller is well tuned for a control system, it is effective to scale ω_o as the sampling rate did for the new ESO to follow system dynamics with different sampling rate since the value of $\omega_o T$ stays unchanged. It is conclude that when GPS sampling rate changes from f to f' , simply enlarge the ESO bandwidth ω_o to ω'_o according to equation

$$\frac{f'}{f} = \frac{\omega'_o}{\omega_o} \tag{18}$$

Then the ESO with new bandwidth parameter ω'_o is adequate to track the parafoil and payload system with GPS sampling rate f' . Other parameters of ADRC may need re-tuned in a small range to adapt the new sampling rate. In the simulation, when GPS sampling rate is 8 Hz, The ADRC parameters for vertical altitude control channel 1 are tuned to be

$$\omega_{o1} = 6, \omega_{c1} = 0.2, b_{01} = 0.02 \tag{19}$$

And the ADRC parameters for horizontal trajectory tracking control channel 2 are tuned to be

$$\omega_{o2} = 6, \omega_{c2} = 0.21, b_{02} = 0.05 \tag{20}$$

The results are shown below.

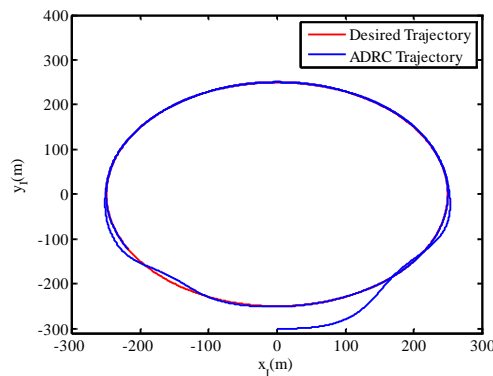


Fig. 7. Horizontal trajectory tracking performance of sampling rate scaled ADRC

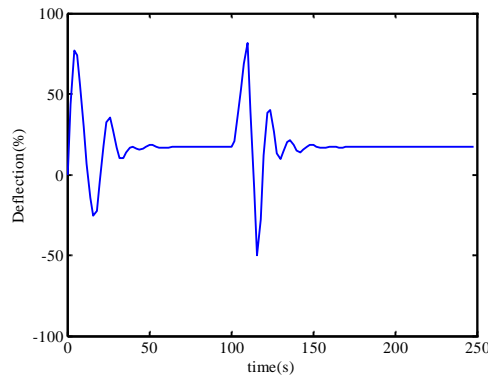


Fig. 8. Deflection output of sampling rate scaled ADRC

Fig. 7 and Fig. 8 are the control performance and output of horizontal ADRC controller. A NASA classical wind gust model is added to the control system as an external disturbance at 100s in the simulation. Fig. 7 shows that the parafoil and payload system tracks the desired path closely until the wind gust is added. The parafoil and payload system flies off the desired trajectory under the impact of wind gust, and the ADRC works rapidly to reject the disturbance. Fig. 8 reveals the procedure of how ADRC works.

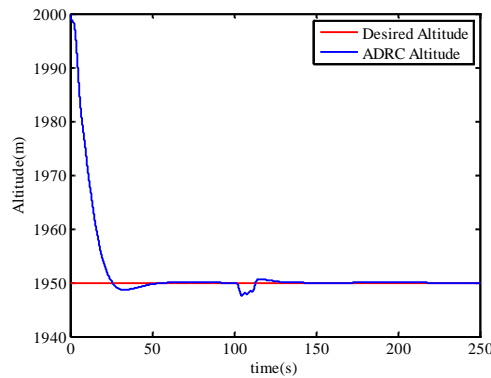


Fig. 9. Vertical altitude tracking performance of sampling rate scaled ADRC

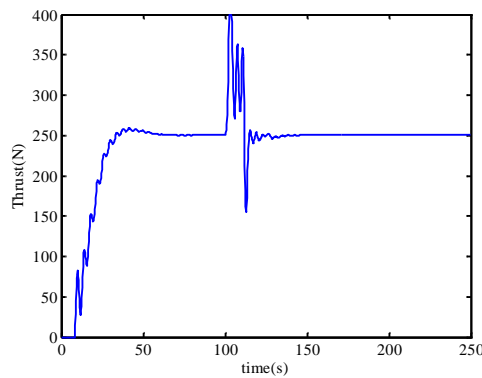


Fig. 10. Thrust output of sampling rate scaled ADRC

Fig. 9 and Fig. 10 show the performance of altitude maintenance and thrust control sequence, respectively. The wind gust added to the system at 100s affects the dynamics and the altitude of the parafoil and payload system. And it is obvious that the ADRC is sufficient for the scaled sampling rate system in trajectory tracking.

5 Conclusion

A new controller based on ADRC algorithm is developed for the parafoil and payload system. It is applied to track the desired horizontal trajectory and vertical altitude. The ADRC controller is model independent, which makes it easier to design. The ESO in ADRC actively estimates the effects of the disturbance on the parafoil and

payload system and makes compensation in real time. This results in a better disturbance rejection performance, as is shown in the simulation results. The comparison with GPC controllers reveals that ADRC outperforms GPC with lower overshoot and less settling time.

In addition, a tuning method of ESO bandwidth ω_o is presented at the end. Simulations prove that the method is effective for trajectory tracking of parafoil and payload system with different sampling rate. The further analysis and mathematical proof are to be studied in the future.

Acknowledgement

The author would like to acknowledge the funding support of the National Natural Science Foundation of China (No.61273138) and the Key Fund of Tianjin (No.14JCZDJC39300).

References

- [1] N. Slegers, A. Brown, J. Rogers, "Experimental investigation of stochastic parafoil guidance using a graphics processing unit," *Control Engineering Practice*, Vol. 38, pp. 27-38, 2015.
- [2] H. Liu, L. Guo, Y.M. Zhang, "An Anti-disturbance PD Control Scheme for Attitude Control and Stabilization of Flexible Space-crafts," *Nonlinear Dynamics*, Vol. 67, No. 3, pp. 2081-2088, 2012.
- [3] V. Devalla, O. Prakash, "Developments in Unmanned Powered Parachute Aerial Vehicle: A Review," *IEEE Aerospace and Electronic Systems Magazine*, Vol. 29, No. 11, pp. 6-20, 2014.
- [4] B.S. Chiel, C. Dever, "Autonomous Parafoil Guidance in High Winds," *Journal of Guidance, Control, and Dynamics*, Vol. 38, No. 5, pp. 963-981, 2015.
- [5] Y.X. Li, Z.Q. Chen, Q.L. SUN, "Flight path tracking of a parafoil system based on the switching between fuzzy control and predictive control," *CAAI Transactions on Intelligent Systems*, Vol. 6, No. 7, pp. 481-488, 2012.
- [6] N. Slegers, M. Costello, "Model predictive control of a parafoil and payload system," *Journal of Guidance, Control, and Dynamics*, Vol. 28, No. 4, pp. 816-821, 2005.
- [7] J.Q. Han, "Active disturbance rejection controller and its applications," *Control and Decision*, Vol. 13, No. 1, pp. 19-23, 1998.
- [8] Y. Huang, W.C. Xue, Z.Q. Gao, H. Sira-Ramirez, D. Wu, M.W. Sun, "Active disturbance rejection control: Methodology, practice and analysis," *ISA Transactions*, Vol. 53, No. 4, pp. 963-976, 2014.
- [9] E.L. Zhu, Q.L. Sun, P.L. Tan, "Modeling of powered parafoil based on Kirchhoff motion equation," *Nonlinear Dynamics*, Vol. 79, No. 1, pp. 617-629, 2015.
- [10] Z.Q. Gao, "Scaling and bandwidth-parameterization based controller tuning," in *Proceedings of 2003 American Control Conference*, pp. 4989-4996, 2003.
- [11] Q. Zheng, L.L. Dong, D.H. Lee, Z.Q. Gao "Active disturbance rejection control for MEMS gyroscopes," *IEEE Transactions on Control Systems Technology*, Vol. 17, No. 6, pp. 1432-1438, 2009.